Epitaxy and Photoresponse of Two-Dimensional GaSe Crystals on Flexible Transparent Mica Sheets

Yubing Zhou,[†] Yufeng Nie,[†] Yujing Liu,[†] Kai Yan,[†] Jinhua Hong,[‡] Chuanhong Jin,[‡] Yu Zhou,[†] Jianbo Yin,[†] Zhongfan Liu,[†,*] and Hailin Peng[†,*]

[†]Center for Nanochemistry, Beijing National Laboratory for Molecular Sciences (BNLMS), State Key Laboratory for Structural Chemistry of Unstable and Stable Species, College of Chemistry and Molecular Engineering, Academy for Advanced Interdisciplinary Studies, Peking University, Beijing 100871, People's Republic of China, and [‡]State Key Laboratory of Silicon Materials, Key Laboratory of Advanced Materials and Applications for Batteries of Zhejiang Province, Department of Materials Science and Engineering, Zhejiang University, Hangzhou 310027, People's Republic of China

ABSTRACT We present the controlled synthesis of high-quality two-dimensional (2D) GaSe crystals on flexible transparent mica substrates *via* a facile van der Waals epitaxy method. Single- and few-layer GaSe nanoplates with the lateral size of up to tens of micrometers were produced. The orientation and nucleation sites of GaSe nanoplates were well-controlled. The 2D GaSe crystal-based photodetectors were demonstrated on both mechanically rigid SiO_2/Si and flexible mica substrates. Efficient photoresponse was observed in 2D GaSe crystal devices on transparent flexible mica substrates, regardless of repeated bending with different radii. The controlled growth of 2D GaSe crystals with efficient photoresponsivity opens up opportunities for both fundamental aspects and new applications in photodetectors.

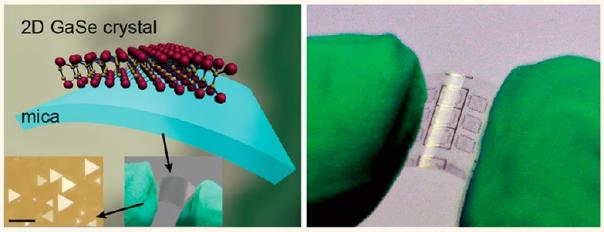

KEYWORDS: gallium selenide · two-dimensional layered crystals · van der Waals epitaxy · optoelectronics

Two-dimensional (2D) layered crystals with highly anisotropic structural, mechanical, optical, and electrical properties have attracted significant attention because of the opportunities they provide to explore unexpected physical and chemical phenomena. The strong intralayer bonding together with the weak interlayer van der Waals interaction in 2D layered crystals facilitates the production and assembly of individual atomic planes, such as graphene,[1,2] hexagonal boron nitride (h-BN),[3,4] and 2D layered chalcogenides. In contrast with zero band gap graphene and insulating h-BN, many 2D layered chalcogenides such as sulfides, selenides, and tellurides are semiconductors, versatile candidates for next generation electronics and optoelectronics applications. Among layered III–VI binary chalcogenides, gallium selenide (GaSe) is an excellent nonlinear optical material and intriguing semiconductor with an indirect band gap of 2.11 eV and a direct band gap of only 25 meV higher,[5−7] which holds promise for optoelectronics,[8,9] nonlinear optics, and terahertz (THz) generation.[10,11]

Layered GaSe has planar tetra-layer (TL) structures with relatively weak interlayer coupling, enabling to be isolated down to a TL. Each TL consists of four atomic planes covalently bonded in the sequence of Se–Ga–Ga–Se (Figure 1A).[9,12] In comparison with their bulk counterparts, 2D crystals of GaSe are expected to have a tunable band gap, high photoresponsivity, and high sensitivity due to the large surface-to-volume ratio and the distinct quantum confinement on their optical and electronic properties.[13,14] The unique 2D geometry, compatible with current microfabrication techniques, also facilitates the fabrication and integration into functional devices. Individual few-layer GaSe nanosheets have been obtained by solvent exfoliation and mechanical cleavage methods and subsequently transferred onto SiO_2/Si substrates for the fabrication of high-performance photodetectors with a fast response and high responsivity.[13] Most recently, few-layer

* Address correspondence to hlpeng@pku.edu.cn, zfliu@pku.edu.cn.

Received for review October 23, 2013 and accepted January 6, 2014.

Published online January 06, 2014
10.1021/nn405529r

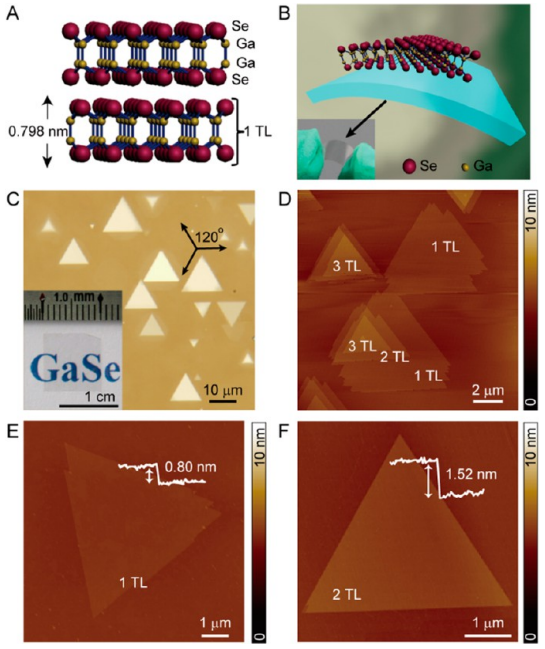

Figure 1. (A) Layered crystal structure of GaSe with each tetra-layer (TL) formed by Se−Ga−Ga−Se atomic sheets. The thickness of 1 TL is about 0.798 nm. (B) Schematic drawing of 2D GaSe crystals grown on a mica substrate *via* van der Waals epitaxy. Inset shows large-area 2D GaSe crystals grown on a transparent flexible mica flake. (C) Typical optical image of ultrathin GaSe nanoplates grown on a mica substrate. Inset shows a photograph of 2D GaSe nanoplate arrays grown on the mica substrate. (D) AFM image of nanoplate array with identical orientations and terrace structures. (E,F) AFM images of nanoplates with thicknesses of 1 TL and 2 TLs, respectively.

GaSe crystals with the thickness down to 2 nm (~2−3 TLs) were successfully synthesized on a rigid SiO_2/Si substrate in a sealed quartz tube by using a vapor phase mass transport method.[15] However, the feasible and controllable synthesis of single- and few-layer GaSe crystals is still desirable.

Here we first demonstrate the growth of 2D GaSe crystals with aligned orientation and specific placement on a transparent flexible mica substrate by van der Waals epitaxy.[16,17] The thickness of 2D GaSe crystals can be controllably reduced to about 0.8 nm, corresponding to 1 TL. The lateral dimensions of 2D GaSe crystals can be up to tens of micrometers. The 2D GaSe crystals show typical a p-type semiconducting behavior. The 2D GaSe photodetectors were fabricated on both rigid SiO_2/Si substrates and flexible transparent mica growth substrates. Efficient photoresponse was observed in 2D GaSe crystal devices on transparent flexible mica substrates even after repeated bending with different radii.

RESULTS AND DISCUSSION

Different from the previously reported metal-catalyzed vapor−liquid−solid (VLS) growth of GaSe nanowires and nanoribbons,[18] 2D GaSe crystals were grown on mica substrates *via* catalyst-free van der Waals epitaxy based on a vapor transport and deposition process inside a tube furnace equipped with a 1 in. diameter quartz tube. The source material, polycrystalline GaSe powder, was placed right at the center region of the tube furnace (790−850 °C). As-produced GaSe vapor was carried downstream by high-purity argon. The substrates, fluorophlogopite mica [$KMg_3(AlSi_3O_{10})F_2$], were placed downstream at the expected locations, where the temperature ranges from 560 to 620 °C. Fluorophlogopite mica with pseudohexagonal Z_2O_5 (Z = Si, Al) layered structure can be cleaved into flexible transparent thin flakes. Remarkably, the thin mica flake provides an ideal atomically smooth and chemically inert surface for van der Waals epitaxy of 2D layered GaSe crystals, allowing for significant lattice mismatch of about 35% between GaSe and mica.[17] The large-area 2D crystals of GaSe grown on flexible transparent insulating mica flakes can serve as a good platform for the measurements of optical and optoelectronic properties (Figure 1B).

The as-grown 2D GaSe crystals on transparent mica substrates were first characterized by their optical contrast in the optical microscope. Figure 1C shows a typical photograph of 2D GaSe crystals grown on mica substrate, featured by triangular shaped GaSe nanoplates with lateral dimensions of several to tens of micrometers. The GaSe nanoplates' edges exhibit identical orientations predominantly at multiples of ~60°, consistent with the 2D hexagonal lattice of the GaSe TL. This observation strongly suggests the epitaxial nature of GaSe crystals on mica. Individual GaSe nanoplates show various optical contrasts related with thicknesses. The ultrathin nanoplates have very flat surfaces, regular shape, and sharp sidewalls. Atomic force microscopy (AFM) was carried out to determine the morphology and thickness of as-grown nanoplates. As shown in Figure 1D, few-layer GaSe nanoplates have identical orientations and terrace structures, which is reminiscent of a layer-by-layer epitaxy mechanism. The height profile of the terrace indicated that the step height of few-layer GaSe is about 0.80 nm, corresponding to the 1 TL thickness of GaSe. Note that individual atomically thin nanoplates with thickness of 1 TL and 2 TLs grown on mica substrates were clearly identified using AFM (Figure 1E,F), which have not been achieved on the SiO_2/Si substrate.[15] The formation of 1 TL thick nanoplates was supposed to be benefited from the strong anisotropic bonding nature of GaSe and the use of atomically smooth mica substrates. Nucleation of 2D GaSe takes place first on the mica surface, followed by lateral covalent bonding of incoming atoms with the atoms at the edge of the nuclei, while the top surface remains passivated by chemically saturated Se atoms. Therefore, the lateral dimension increases much faster than the vertical thickness. In other words, growth anisotropy of 2D GaSe is guaranteed by its strong anisotropy in layered crystal structure. The thickness

of layered GaSe flakes can be tuned by adjusting the growth time, pressure, and Ar gas flow rate. For short growth time (5−20 min), the pressure of 30−50 Torr, and Ar gas flow of 50−70 sccm, we can obtain atomically thin layered GaSe flakes as shown in Figure 1E,F. The thickness distribution of nanoplates was found to be relatively sharp. For example, GaSe nanoplates obtained in a substrate area of 500 μm × 500 μm exhibited a thickness of mainly 1 TL (Supporting Information Figure S1). Furthermore, we prepared slightly thick GaSe flakes with large area or thin films with lateral dimensions extending from several micrometers up to hundreds of micrometers using longer growth time (30−60 min), Ar gas flow (70−100 sccm), and moderate pressure (10−30 Torr). As shown in Figure S2, the lateral dimension of 2D GaSe crystals was found to reach ~0.1 mm, which can eventually coalesce to form 2D nanoplate aggregates and even a large-size continuous film on mica. We showed the detailed influence of the pressure as an example when the other conditions in Figure S3 were fixed. With the decrease of the pressure, the thickness distribution has a tendency to increase.

Transmission electron microscopy (TEM) was used to characterize the microstructure and chemical composition of the 2D GaSe crystals. Free-standing GaSe nanoplates were transferred from the mica substrate to a TEM grid with the assistance of a drop of dilute HF solution (2% v/v). Figure 2A shows a typical low-magnification TEM image of ultrathin GaSe nanosheets supported by the holey carbon film. The ultrathin GaSe nanosheets are relatively stable against the electron-beam irradiation in a TEM operated at 300 kV. The high-resolution TEM (HRTEM) image and fast Fourier transformation (FFT) pattern demonstrate that the ultrathin nanosheet is of single-crystalline hexagonal phase. As shown in Figure 2B, the lattice spacing between the planes was measured to be 0.323 nm, corresponding to the (10−10) lattice plane of hexagonal GaSe. The FFT pattern exhibits a single set of hexagonally symmetric pattern, confirming the single-crystalline nature (Figure 2B, inset). Similar with GaSe nanowires synthesized by VLS growth, the nanoplates grow along the [11−20] direction. Figure 2C shows a folded edge of a GaSe nanoplate. The close-up view of the folded edge of the nanoplate reveals that the nanoplate can be easily bent to ~180° with a radius of less than 5 μm without fracture. From the HRTEM image in Figure 2C, a 5 TL thick structure with alternating bright and dark fringes is clearly visible. The periodic spacing of these fringes is ~0.798 nm, corresponding to the periodicity of stacked GaSe TLs. We also characterized the individual GaSe nanoplate using high-angle annular dark-field (HAADF) imaging (Figure 2D). The corresponding element mapping images indicate that Ga and Se elements are uniformly distributed, confirming uniform chemical composition along the entire nanoplate with a Ga/Se atomic ration of 1:1 (Figure 2E,F).

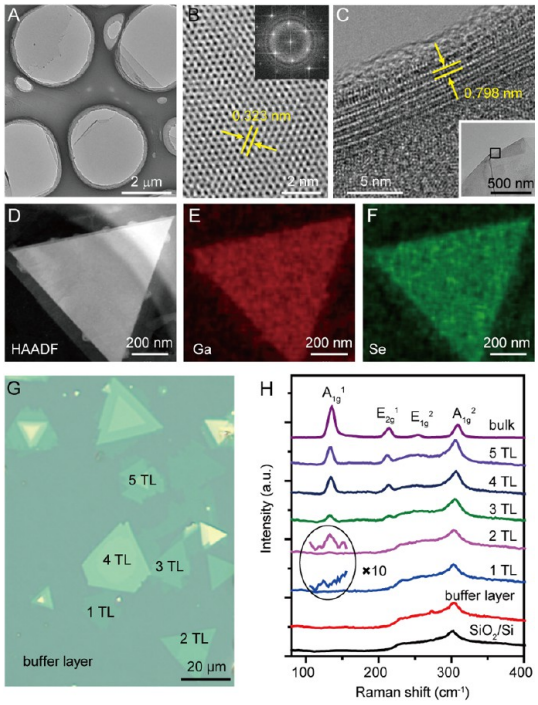

Figure 2. TEM and Raman spectroscopy characterizations of 2D GaSe crystals. (A) Low-magnification TEM image of a 2D GaSe crystal. (B) Typical HRTEM image obtained from the same crystal shown in (A). Inset: corresponding fast Fourier transformation (FFT) pattern. (C) HRTEM image of a folded edge of the 2D GaSe crystal. The layered structures with periodical fringes indicate the layer number. Recording position is from the black square in the inset. (D) High-angle annular dark-field imaging (HAADF) of a 2D GaSe crystal. (E,F) Ga and Se element maps of the corresponding GaSe crystal, respectively. (G) Optical image of 2D GaSe crystals on SiO_2/Si substrate. (H) Layer-number-dependent Raman spectra of 2D GaSe crystals. The Raman intensity of the bulk GaSe was reduced 10 times.

To study the structure and quality of 2D GaSe crystals, we have also carried out detailed Raman spectroscopy for 2D GaSe crystals with different layers. A typical Raman spectrum of bulk GaSe consists of characteristic peaks for the A_{1g}^1 mode (133.0 cm^{-1}), E_{2g}^1 mode (211.9 cm^{-1}), E_{1g}^2 mode (250.0 cm^{-1}), and A_{1g}^2 mode (306.8 cm^{-1}),[19−22] which have overlaps with the Raman peaks of mica substrates. Two A_{1g} modes correspond to the out-of-plane vibrational mode of the Se−Ga−Ga−Se lattice, while E_{1g} and E_{2g} associate with the in-plane vibrational mode. Figure 2G shows a typical optical image of 2D GaSe crystals grown directly on a SiO_2/Si substrate. AFM measurements revealed that the thicknesses of 2D GaSe crystals ranged from 1 TL to 5 TLs. Figure 2H plots the evolution of Raman spectra for a 514 nm excitation as a function of the number of GaSe layers. In the GaSe monolayer, the Raman mode of A_{1g}^2 at 302.6 cm^{-1} was shifted at room temperature; however, the Raman vibrational modes at A_{1g}^1, E_{2g}^1, and E_{1g}^2 are very weak and their

peaks are invisible. The intensities of the Raman modes are observed to decrease with reducing layer thickness for GaSe. As shown in Figure S4, the map of A_{1g}^1 band intensity has a uniformly distributed color, indicating the structural integrity and uniformity of the GaSe nanoplate within the Raman spatial resolution of $\sim$1 μm.

In additional to orientation, thickness, and structure control, we succeeded in position control of GaSe nanoplates, which is crucial for subsequent integration of as-grown nanostructures into practical devices. Generally, the initial nucleation of GaSe nanoplates is totally random on the atomically flat surface of mica. However, once the nucleation of the GaSe nanoplate is positioned on selectively modified mica substrates, the subsequent growth of nanoplates could be locally confined. To this end, we utilized selective oxygen plasma etching to modify specific regions of the mica surface with PMMA lithography masks according to the method described in our previous work.[23] As-prepared mica substrates were loaded into a tube furnace for the GaSe flake growth. Dramatic changes in both topography and chemical composition of mica were introduced upon selective area plasma etching, resulting in referred nucleation and growth of GaSe nanoplates on the intact mica regions rather than the etched regions. Typical growth results of GaSe nanoplates and membranes with various patterns according to the photolithography templates are shown in Figure 3A–D. Well-ordered 4 $\times$ 5 arrays of triangular, hexagonal, round, and perforated GaSe nanoplates were created on the mica surface. Even more complicated pattern can also be readily obtained by using this selective area growth technique.

Electrical transport properties and the photoresponse behavior of individual 2D GaSe crystals were further studied. After transferring the GaSe nanoplates onto 300 nm thick SiO_2/Si substrate, we fabricated field-effect transistor (FET) devices by standard e-beam lithography and thermal evaporation of 5 nm Ti/70 nm Au contacts. The room-temperature gate-voltage-dependent transport measurements were carried out by applying a drain-source voltage (V_{ds}) to a pair of Ti/Au pattern electrodes and gate voltage (V_g) to the back gate silicon substrate electrode. The 2D GaSe crystals were found to show a typical p-type semiconducting behavior (data shown in Figure S5A,B). Figure 4A shows the $I-V$ characteristics of an ultrathin GaSe nanoplate (about 6 nm in thickness) in the dark and in the presence of visible light (a 150 W halogen lamp, light energy density of about 3.3 mW/cm^2), which indicate a pronounced photoconducting response of 2D GaSe crystals on SiO_2/Si substrates. A stable and repeatable operation of dynamic photoresponse was observed in the 2D GaSe crystal. As shown in Figure 4B, with light illumination off and on, the current exhibited a "low" dark current of

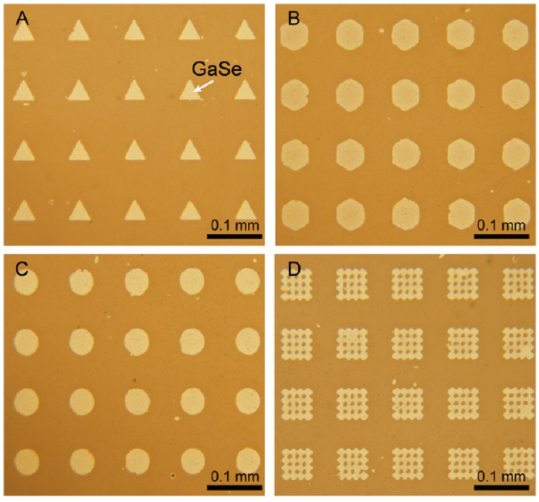

Figure 3. (A–D) Optical images of triangular, hexagonal, round, and perforated GaSe plate arrays obtained by the site-controlled growth, respectively.

$\sim$1.3 pA and a "high" current of $\sim$148.8 pA when the device is biased at 10 V, respectively. The on/off switching ratio averaged over 20 devices was calculated to be as high as 110. Meanwhile, the switching time between the on/off states was found to be shorter than the current measuring time of the equipment. Given the incident light intensity of 3.27 mW/cm^2, the active area of $\sim$7.5 μm^2, the measured current of 148 pA, the photosensitivity of the 2D GaSe crystal on the SiO_2/Si substrate is calculated to be about 0.6 A/W, which is superior to the previously reported photosensitivity of the few-layer GaSe flake grown recently by vapor-phase mass transport (17 mA/W with a bias of 10 V)[15] and comparable to the value of mechanically exfoliated 2D GaSe flakes ($\sim$2.8 A/W).[13] We have also carried out the measurements to reveal the long-term operation and possible aging effects of GaSe flake devices (data shown in Figure S5C). Moreover, the output photocurrent decreased linearly as incident light power declined (Figure S5D), which suggests that the photocurrent is solely determined by the amount of photogenerated carriers under illumination.

The use of dielectric mica growth substrates is compatible with conventional photolithographic process, which facilitates the transfer-free batch fabrication of GaSe nanoplate devices and avoids potential damage during the transfer process of the nanoplate. We used standard photolithography for direct fabrication of devices based on as-grown 2D GaSe crystals. Ti/Au (5 nm/70 nm) was deposited on the flexible and insulating mica substrate as the electrodes with a channel width of 8 μm. A typical photograph and optical image of the device array are shown in Figure 4C,D, respectively. To investigate the durability of the flexible photodetector based on 2D GaSe crystals, the photoresponse of the devices made on

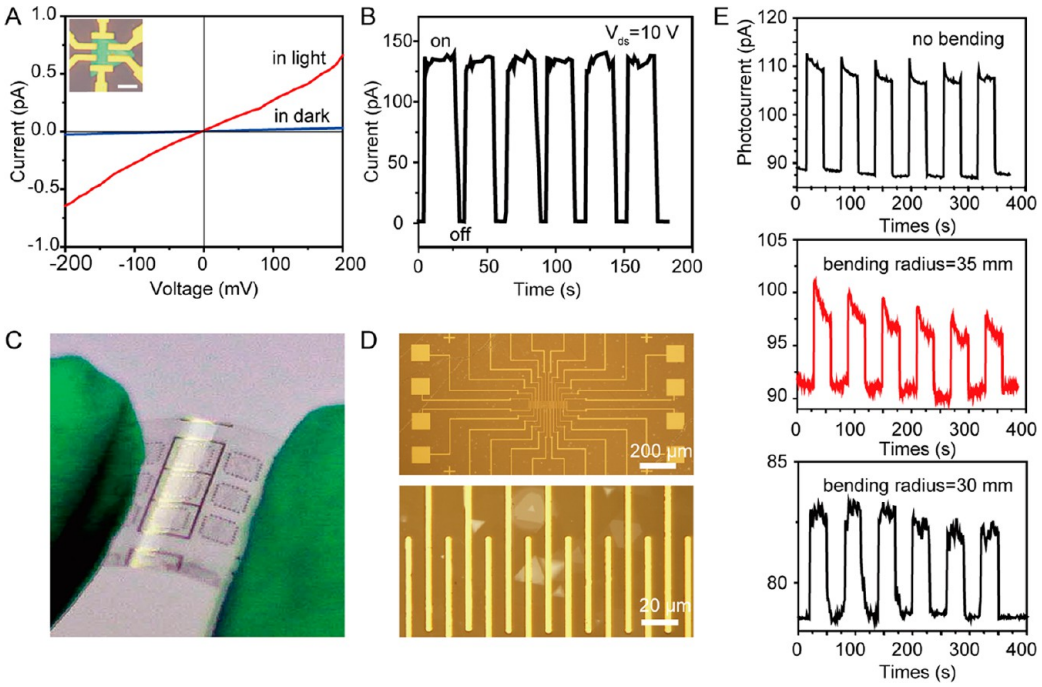

Figure 4. Electronic and photoresponse properties of 2D GaSe crystals. (A) *I*−*V* characteristics in the dark and in the presence of white light for GaSe nanoplate. Inset: optical micrograph of an individual 2D GaSe crystal device made by e-beam lithography. Scale bar: 5 μm. (B) Photocurrent as a function of time at the bias voltage of 10 V, on/off switching ratio = ∼110. (C) Photograph of a patterned device array composed of a GaSe nanoplate on a transparent mica substrate. (D) Optical microscopy image of the GaSe nanoplate device arrays. (E) Time trace of source-drain current when visible light was toggled on and off before and after bending to different bending radii at bias voltage of 10 V.

mica substrates was measured before/after repeated bending with different radii. Figure 4E plots the photoresponse *versus* time characteristics of the devices exposed to an on/off light illumination after repeated bending of mica substrates with the bending radii of 35 and 30 mm, respectively. The slight decrease of on/off switching ratio was observed during reducing of the bending radius. The photocurrent and responsivity of the GaSe photodetectors both declined upon bending, in agreement with the decrease in effective irradiance. It was also noted that devices with Au electrodes exhibited improved contact resistance in comparison with devices with Ti/Au electrodes. The measured photoresponsivity of 2D GaSe crystal devices on transparent flexible mica substrates is about 30 mA/W, which is superior to the previously reported photoresponsivity of pristine graphene (∼1 mA/W)[24,25] and single-layer MoS_2 (∼7.5 mA/W).[26]

CONCLUSIONS

In summary, we succeeded in controllable synthesis of single-crystalline ultrathin GaSe nanoplates on a flexible mica substrate *via* van der Waals epitaxy. GaSe nanoplates with uniform thickness down to 1 TL and lateral dimension up to tens of micrometers were obtained. The control of the orientation and nucleation of GaSe nanoplates has been achieved. Large-area continuous GaSe nanosheet film can also be obtained by tuning growth conditions. Individual 2D GaSe nanoplates were found to show typical p-type conductance and good light response characteristics. Furthermore, efficient photoresponse was observed on 2D GaSe crystal devices directly fabricated on flexible mica substrates even after repeated bending with different radii. The controlled synthesis of 2D GaSe crystals provides a promising material for applications in novel photodetectors.

EXPERIMENTAL SECTION

Synthesis of the GaSe Source. The GaSe source was prepared with high-purity gallium and selenium, *via* a modified Bridgman method. Gallium was mixed with selenium at the molar ratio of 1:1 and then sealed in an evacuated quartz tube under the pressure of $<5 \times 10^{-2}$ Pa. The mixture was heated to 1050 °C for 6 h. Then the system was cooled to 960 °C in 1 h followed by natural cooling. The obtained red-brown GaSe polycrystalline compound semiconductor has a diverse morphology, but most of them have triangular layered structures with mica-like stacking form.

Characterization of Monolayer and Few-Layer GaSe. The morphology and structure of the synthesized nanomaterials were characterized by optical microscopy (OM, Olympus DX51), scanning electron microscopy (SEM, Hitachi S-4800), atomic force microscopy (AFM, Digital Instrument Nanoscope IIIA), transmission electron microscopy (TEM, FEI Tecnai F30), and micro-Raman spectroscopy (Horiba, LabRAM HR-800).

Conflict of Interest: The authors declare no competing financial interest.

Acknowledgment. We acknowledge financial support by the National Natural Science Foundation of China (Nos. 21173004, 21222303, 51121091, 51290272, and 51222202), the National Basic Research Program of China (Nos. 2011CB921904, 2013CB932603, 2014CB932500, and 2012CB933404), the Fundamental Research Funds for the Central Universities (No. 2012QNA4005), NCET, and SRF for ROCS, SEM.

Supporting Information Available: Additional experimental details and figures. This material is available free of charge *via* the Internet at http://pubs.acs.org.

REFERENCES AND NOTES

1. Novoselov, K. S.; Geim, A. K.; Morozov, S. V.; Jiang, D.; Zhang, Y.; Dubonos, S. V.; Grigorieva, I. V.; Firsov, A. A. Electric Field Effect in Atomically Thin Carbon Films. *Science* **2004**, *306*, 666–669.
2. Novoselov, K. S.; Jiang, D.; Schedin, F.; Booth, T. J.; Khotkevich, V. V.; Morozov, S. V.; Geim, A. K. Two-Dimensional Atomic Crystals. *Proc. Natl. Acad. Sci. U.S.A.* **2005**, *102*, 10451–10453.
3. Lipp, A.; Schwetz, K. A.; Hunold, K. Hexagonal Boron Nitride: Fabrication, Properties and Applications. *J. Eur. Ceram. Soc.* **1989**, *5*, 3–9.
4. Alem, N.; Erni, R.; Kisielowski, C.; Rossell, M. D.; Gannett, W.; Zettl, A. Atomically Thin Hexagonal Boron Nitride Probed by Ultrahigh-Resolution Transmission Electron Microscopy. *Phys. Rev. B* **2009**, *80*, 155425.
5. Mooser, E.; Schlüter, M. The Band-Gap Excitons in Gallium Selenide. *Nuovo Cimento B* **1973**, *18*, 164–208.
6. Wieting, T. J. *Electrons and Phonons in Layered Crystal Structures*; D. Reidel: Dordrecht, The Netherlands, 1979; Vol. 3.
7. Capozzi, V.; Montagna, M. Optical Spectroscopy of Extrinsic Recombinations in Gallium Selenide. *Phys. Rev. B* **1989**, *40*, 3182–3190.
8. Leontie, L.; Evtodiev, I.; Nedeff, V.; Stamate, M.; Caraman, M. Photoelectric Properties of Bi_2O_3/GaSe Heterojunctions. *Appl. Phys. Lett.* **2009**, *94*, 071903.
9. Fernelius, N. C. Properties of Gallium Selenide Single-Crystal. *Prog. Cryst. Growth Charact. Mater.* **1994**, *28*, 275–353.
10. Shi, W.; Ding, Y. J. J.; Fernelius, N.; Vodopyanov, K. Efficient, Tunable, and Coherent 0.18−5.27-THz Source Based on GaSe Crystal. *Opt. Lett.* **2002**, *27*, 1454–1456.
11. Kubler, C.; Huber, R.; Tubel, S.; Leitenstorfer, A. Ultrabroadband Detection of Multi-Terahertz Field Transients with GaSe Electro-optic Sensors: Approaching the Near Infrared. *Appl. Phys. Lett.* **2004**, *85*, 3360–3362.
12. Bube, R. H.; Lind, E. L. Photoconductivity of Gallium Selenide Crystals. *Phys. Rev.* **1959**, *115*, 1159–1164.
13. Hu, P. A.; Wen, Z. Z.; Wang, L. F.; Tan, P. H.; Xiao, K. Synthesis of Few-Layer GaSe Nanosheets for High Performance Photodetectors. *ACS Nano* **2012**, *6*, 5988–5994.
14. Late, D. J.; Liu, B.; Luo, J. J.; Yan, A. M.; Matte, H. S. S. R.; Grayson, M.; Rao, C. N. R.; Dravid, V. P. GaS and GaSe Ultrathin Layer Transistors. *Adv. Mater.* **2012**, *24*, 3549–3554.
15. Lei, S.; Ge, L.; Liu, Z.; Najmaei, S.; Shi, G.; You, G.; Lou, J.; Vajtai, R.; Ajayan, P. M. Synthesis and Photoresponse of Large GaSe Atomic Layers. *Nano Lett.* **2013**, *13*, 2777–2781.
16. Koma, A. Vanderwaals Epitaxy: A New Epitaxial-Growth Method for a Highly Lattice-Mismatched System. *Thin Solid Films* **1992**, *216*, 72–76.
17. Koma, A. Van der Waals Epitaxy for Highly Lattice-Mismatched Systems. *J. Cryst. Growth* **1999**, *201*, 236–241.
18. Peng, H. L.; Meister, S.; Chan, C. K.; Zhang, X. F.; Cui, Y. Morphology Control of Layer-Structured Gallium Selenide Nanowires. *Nano Lett.* **2007**, *7*, 199–203.
19. Balitskii, O. A.; Savchyn, V. P.; Yukhymchuk, V. O. Raman Investigation of InSe and GaSe Single-Crystals Oxidation. *Semicond. Sci. Technol.* **2002**, *17*, L1.
20. Kulibekov, A. M.; Olijnyk, H. P.; Jephcoat, A. P.; Salaeva, Z. Y.; Onari, S.; Allakhverdiev, K. R. Raman Scattering under Pressure and the Phase Transition in ε-GaSe. *Phys. Status Solidi B* **2003**, *235*, 517–520.
21. Wieting, T. J.; Verble, J. L. Interlayer Bonding and the Lattice Vibrations of β-GaSe. *Phys. Rev. B* **1972**, *5*, 1473–1479.
22. Ibragimov, T. D.; Kurbanova, G. G.; Gorelik, V. S. Raman Scattering in Gallium Selenide and Sulfide Films. *Phys. Status Solidi B* **1989**, *155*, 113–116.
23. Li, H.; Cao, J.; Zheng, W. S.; Chen, Y. L.; Wu, D.; Dang, W. H.; Wang, K.; Peng, H. L.; Liu, Z. F. Controlled Synthesis of Topological Insulator Nanoplate Arrays on Mica. *J. Am. Chem. Soc.* **2012**, *134*, 6132–6135.
24. Xia, F. N.; Mueller, T.; Lin, Y. M.; Valdes-Garcia, A.; Avouris, P. Ultrafast Graphene Photodetector. *Nat. Nanotechnol.* **2009**, *4*, 839–843.
25. Xia, F.; Mueller, T.; Golizadeh-Mojarad, R.; Freitag, M.; Lin, Y.-m.; Tsang, J.; Perebeinos, V.; Avouris, P. Photocurrent Imaging and Efficient Photon Detection in a Graphene Transistor. *Nano Lett.* **2009**, *9*, 1039–1044.
26. Yin, Z. Y.; Li, H.; Li, H.; Jiang, L.; Shi, Y. M.; Sun, Y. H.; Lu, G.; Zhang, Q.; Chen, X. D.; Zhang, H. Single-Layer MoS_2 Phototransistors. *ACS Nano* **2012**, *6*, 74–80.